Published in final edited form as:
Dev Biol. 2008 July 15; 319(2): 201–210. doi:10.1016/j.ydbio.2008.03.043.

TSKS Concentrates in Spermatid Centrioles During Flagellogenesis

Bingfang Xu,
Center for Research in Contraceptive and Reproductive Health, Department of Cell Biology, University of Virginia, Charlottesville, VA 22908

Zhonglin Hao,
Center for Research in Contraceptive and Reproductive Health, Department of Cell Biology, University of Virginia, Charlottesville, VA 22908

Kula N. Jha,
Center for Research in Contraceptive and Reproductive Health, Department of Cell Biology, University of Virginia, Charlottesville, VA 22908

Zhibing Zhang,
Department of Obstetrics & Gynecology, Virginia Commonwealth University, Richmond, VA, 23298

Craig Urekar,
Center for Research in Contraceptive and Reproductive Health, Department of Cell Biology, University of Virginia, Charlottesville, VA 22908

Laura Digilio,
Center for Research in Contraceptive and Reproductive Health, Department of Cell Biology, University of Virginia, Charlottesville, VA 22908

Silvia Pulido,
Center for Research in Contraceptive and Reproductive Health, Department of Cell Biology, University of Virginia, Charlottesville, VA 22908

Jerome F Strauss III,
Department of Obstetrics & Gynecology, Virginia Commonwealth University, Richmond, VA, 23298

Charles J. Flickinger, and
Center for Research in Contraceptive and Reproductive Health, Department of Cell Biology, University of Virginia, Charlottesville, VA 22908

John C. Herr
Center for Research in Contraceptive and Reproductive Health, Department of Cell Biology, University of Virginia, Charlottesville, VA 22908

Abstract

Centrosomal coiled-coil proteins paired with kinases play critical roles in centrosomal functions within somatic cells, however knowledge regarding gamete centriolar proteins is limited. In this study, the substrate of TSSK1 & 2, TSKS, was localized during spermiogenesis to the centrioles of post-meiotic spermatids, where it reached its greatest concentration during the period of flagellogenesis. This centriolar localization persisted in ejaculated human spermatozoa, while centriolar TSKS diminished in mouse sperm, where centrioles are known to undergo complete

Corresponding author: John C. Herr, Center for Research in Contraceptive and Reproductive Health, Department of Cell Biology, University of Virginia, 1300 Jefferson Park Avenue, Charlottesville, VA 22908; Tel. 434 924 2007; E-Mail: E-mail: jch7k@virginia.edu.

degeneration. In addition to the centriolar localization during flagellogenesis, mouse TSKS and the TSSK2 kinase localized in the tail and acrosomal regions of mouse epididymal sperm, while TSSK2 was found in the equatorial segment, neck and the midpiece of human spermatozoa. TSSK2/TSKS is the first kinase/substrate pair localized to the centrioles of spermatids and spermatozoa. Coupled with the infertility due to haploinsufficiency noted in chimeric mice with deletion of TSSK 1 & 2 (companion paper) this centriolar kinase/substrate pair is predicted to play an indispensable role during spermiogenesis.

Keywords

TSSK2; TSKS; Centriole; Spermatid; Spermatozoa; Spermiogenesis; Flagellogenesis

Introduction

In early spermiogenesis the spermatid centrosome consists of a pair of cylindrical centrioles and pericentriolar centrosomal proteins. As spermiogenesis progresses the distal centriole serves as a nucleation site for development of the axonemal microtubules which comprise the central core of the sperm flagellum (Fawcett 1970). During flagellogenesis processes, intramanchette transport (IMT) and intraflagellar transport (IFT) convey cargo proteins in the raft protein complexes that mobilize along microtubules, thus delivering building blocks for sperm tail assembly through the action of molecular motors (Kierszenbaum 2001, 2002, Marshall 2007). During these transport processes the centriole/basal body recruits flagellar/ciliary assembly factors (Deane *et al.* 2001), and serves as a site where “cargo” is loaded for its journey out to the flagellar/ciliary tip.

Universal observations in mammalian development are “reduction” of the gamete's centrosome during gametogenesis followed by centrosome “restoration” during fertilization (Schatten 1994, Sutovsky and Schatten 2000). Centrosome reduction during spermiogenesis refers to a gradual centrosomal inactivation involving partial or full degeneration, depending on the species (Manandhar *et al.* 2000a). In non-rodents, mammalian spermatozoa centrosomes degenerate only partially. In human sperm, for example, the proximal centriole remains fully intact, while the distal centriole degenerates and 50% of its microtubule triplets are lost (Manandhar *et al.* 2000b). By contrast, in caudal epididymal spermatozoa of mice and rats, centrioles undergo complete degeneration (are morphologically unrecognizable) and centrosomal proteins such as γ-tubulin and centrin become undetectable (Manandhar *et al.* 2005).

Centrosomal reduction does not impair gamete functions during fertilization, but the process is significant for patterns of centrosomal inheritance (Schatten 1994). A current model of centrosome behavior during fertilization in higher animals holds that the sperm introduces partially degenerated centrioles into the ooplasm. After a quiescent period, sperm centrioles recruit oocyte centrosomal proteins which have dispersed but are readily available in the ooplasm, due to the previous complete degeneration of oocyte centrioles (Manandhar *et al.* 2005).

In *C. elegans*, the recruitment of the centrosomal proteins by sperm centrioles is the starting event leading to establishment of polarity during early embryogenesis (Cowan and Hyman 2006). It is assumed that in higher animals, the degeneration of the gamete centrosome and its re-assembly in the ooplasm may also control the initiation of cleavage and early embryonic development. Since the spermatozoa of several species (e.g. rodents) lack centrioles due to complete centriolar degeneration, centrioles may originate *de novo* in the ooplasm without being associated with pre-existing centrioles. Therefore, in these species, sperm centrioles may

not be essential for early cleavage even though the persistence of sperm centrioles in most other species is considered the more conservative, generalized pathway that allows fertilization and early development to be more efficient (Manandhar *et al.* 2005, Nakamura *et al.* 2005).

Centrosome/basal body proteins have been studied by proteomic analyses in the green alga *Chlamydomonas reinhardtii* (Keller *et al.* 2005), human (Andersen *et al.* 2003) and yeast (Wigge *et al.* 1998). Two striking features have been found. First, numerous basal body proteins are encoded by genes that are up-regulated during flagellar assembly, implying a role of basal bodies in ciliogenesis-related functions. Second, structural analyses of human centrosomal proteins reveal that a high proportion (75%) contain coiled-coil regions, although few have any other recognizable motifs or domains (Andersen *et al.* 2003). A similar observation has been made by structural analysis of yeast spindle pole body proteomes. Of the 27 proteins localized to the yeast spindle pole region, 19 are potential coiled-coil proteins, raising the intriguing question how various coiled-coil proteins interact to form the pericentriolar and centriolar matrix (Wigge *et al.* 1998).

Several centrosomal coiled-coil proteins have been found to interact with kinases which are essential for centrosomal maturation, duplication and cell division. In *C. elegans*, the coiled-coil centrosomal proteins SPD-2, SAS-4, SAS-5, and SAS-6 interact with Aurora-A and ZYG-1 kinases (Kemp *et al.* 2004, Hamill *et al.* 2002). *Drosophila* centrosomal protein TACC (transforming acidic coiled-coil) is the substrate of Aurora-A kinase (Giet *et al.* 2002, Barros *et al.* 2005, Le Bot *et al.* 2003). In human cell lines several centrosomal coiled-coil protein/kinase pairs have been studied including: ninein with glycogen synthase kinase 3β (GSK-3β) (Hong *et al.* 2000); Cep55 with Erk2/Cdk1 and Plk1 (Fabbro *et al.* 2005); AKAP450 and pericentrin with protein kinase A and protein kinase CK1 (Gillingham and Munro 2000, Keryer *et al.* 2003, Sillibourne *et al.* 2002); ODF2 with Plk1 (Soung *et al.* 2006); and C-Nap1 with Nek2A kinase, which itself has a coiled-coil domain (Fry *et al.* 1998).

The substrate of testis specific serine kinase 1 and 2, TSKS, has two coiled-coil regions. In yeast two hybrid studies, full length human TSKS strongly bound TSSK2 with a strength 1.5 times that between large T antigen and p53 (Hao *et al.* 2004). In the preceding companion paper, analysis of TSKS deletion mutants revealed that the N-terminus of TSKS is essential for TSSK2 interaction. Moreover, targeted deletion of *TSSK1 & 2* resulted in infertility due to haploinsufficiency, and both human and mouse TSKS were strongly phosphorylated by TSSK2. In the present study, TSKS was localized in spermatid centrioles, where it reached its greatest concentration during the period of flagellogenesis. This centriolar localization persisted in ejaculated human spermatozoa, while centriolar TSKS diminished in mouse sperm which undergo complete centriolar degeneration. TSSK2/TSKS is the first kinase/substrate pair localized to the spermatid centrioles. It is posited that the coiled-coil region of TSKS is related to its centriolar localization, and through its binding activity with TSKS, TSSK2 is recruited to the spermatid centrioles to fulfill its essential function.

Materials and Methods

In situ hybridization

Testes were collected from normal adult mice and fixed in paraformaldehyde (4%). Following dehydration, the blocks were embedded in paraffin, sectioned and mounted on slides. To prepare riboprobes, the full length cDNAs of mouse TSKS and TSSK2 were subcloned into the pBluescript SK vector and used as templates for *in vitro* transcription. Tritiated uridine triphosphate (UTP) was incorporated into the sense or antisense riboprobes by either T3 or T7 RNA polymerase. A labeled β-actin riboprobe was used as a positive control. The sections were deparaffinized, rehydrated, treated with proteinase K and incubated in *in situ* hybridization solution described by Stoler (1990). The final probe concentrations were

normalized for probe length and applied at full saturation (0.2 μg/ml/kilobase (kb) complexity). Hybridization was carried out at 55-65°C. After hybridization, the sections were washed under high-stringency conditions to remove non-specific hybridization. The slides were overlaid with autoradiograhic emulsion, exposed 2-4 weeks at 4°C, developed photographically, and lightly counterstained with hematoxylin and eosin.

Preparation of enzyme-dissociated testicular cells, testis cryosections and spermatozoa

Preparation of enzyme-dissociated testicular cells—Samples of human testis were obtained from surgical specimens. Normal adult mouse testes were collected after decapitation. The tissues were minced into small blocks and dissociated with 0.5 mg/ml collagenase and 0.1 Units/ml micrococcal nuclease at 33°C for 0.5-1 hr. Dissociated cells were washed by PBS and fixed for 20 min with 4% paraformaldehyde. Cells were then washed again by PBS and air dried on slides.

Preparation of testis cryosections—Normal adult mouse testes were fixed in 4% paraformaldehyde for 24 hrs, then cryosectioned and stored at -70°C for later use.

Preparation of "swim-up", capacitated and acrosome-reacted spermatozoa—Freshly ejaculated human semen samples were liquefied for 0.5-1 hr at 22°C. Then 0.25 ml semen was carefully overlaid with 2 ml BWW medium. The samples were then incubated at 37°C for 1 hr to allow the sperm to swim up. The upper half of the "swim-up" sperm fraction was carefully transferred to a fresh tube without disturbing the lower half. These "swim-up" sperm were collected by centrifuging at 600 × g for 10 min, re-suspended at a concentration of 20×10^6 sperm/ml in BWW medium that contained 30 mg/ml of human serum albumin (HSA), and capacitated at 37 °C overnight in a CO_2 incubator. Following incubation in capacitating medium, progesterone in absolute ethanol was added to one group at a final concentration of 5μM, while an equal volume of ethanol alone was added to the control group, and the acrosome-reaction was induced by incubation for 30 min at 37 °C in a CO_2 incubator. PSA lectin staining was conducted to identify sperm that had undergone the acrosome reaction. Aliquots of "swim-up", capacitated and acrosome-reacted sperm were spotted and onto poly-L-lysine-coated glass slides after washing with PBS and adjusting the sperm concentration and were air-dried. Preparations of mouse sperm were obtained using the protocol described by Jha *et al.* (2006).

Immunofluorescence

For immunofluorescence microscopy, sample slides were fixed with 4% paraformaldehyde for 10 min. Following PBS washing, the slides were either incubated in 1% Triton X-100 for 5 min at 37 °C or incubated in -20 °C methanol for 5 min to permeabilize the membranes and increase antibody access. After permeabilization, the slides were washed with PBS, and blocked in 10% normal goat serum with PBS for 0.5-2 hrs. For primary antibody staining, the slides were incubated in PBS with 1-3% BSA, 1:150 rat anti-TSKS serum, 1: 250 rabbit anti-TSSK2 serum, or the corresponding preimmune-serum overnight at 4 °C. Following washing with PBS, the slides were incubated in PBS with 1% BSA and secondary immunoreagents (Jackson ImmunoResearch) at 1:200 dilution for 1 hr. Finally, the slides were washed with PBS, coated with SlowFade Gold Antifade reagent containing 4′,6′-diamidino-2-phenylindole dihydrochloride (DAPI) (Molecular Probes, Eugene, OR) for nuclear staining, mounted under coverslips, and viewed in a Zeiss Axiovert 200 inverted fluorescent microscope equipped with epifluorescence and a digital camera using Open Lab software.

Antibodies against α-tubulin, γ-tubulin, and the centrosomal protein, Cep57 (KIAA 0092), were employed to localize these proteins along with TSKS in "swim-up" human spermatozoa. Details of these immunoreagents include: mouse monoclonal anti-γ-tubulin (Abcam, Cat#

ab11316, working dilution at 1:50 or 1:100 in PBS with 3% BSA); mouse anti-Cep57 (hybridoma supernatant from Dr. Momotani from University of Virginia, working dilution at 1:25 or 1:50 in PBS with 3% BSA); and monoclonal anti-α-tubulin (Sigma, mouse monoclonal DM1A, Production No. T6199, working concentration 10μg/ml in PBS with 3% BSA).

Results

Post-meiotic expression of TSSK2 and TSKS mRNAs

Testis-specific expression of *TSSK2* and *TSKS* mRNA has been reported previously by Northern and dot blot methods (Hao *et al.* 2004, Kueng *et al.* 1997). In order to understand the temporal appearance of *TSSK2* and *TSKS* messages during spermatogenesis, *in situ* hybridization was performed using radiolabeled cRNAs on mouse testis. In Fig. 1A-D, seminiferous tubules hybridized with antisense TSSK2 are shown marked in the tubule lumen with numbers indicating the stage of the cycle of the seminiferous epithelium. In Fig. 1A and B, silver grains indicating *TSSK2* transcripts were concentrated predominately in the adluminal layers of the seminiferous tubules. Comparison of tissue morphology in higher magnification (×400) bright-field preparations stained with hematoxylin and eosin to the locations of silver grains resolved in dark field images revealed *TSSK2* transcripts mainly in the post-meiotic spermatids (red arrows), while labeling of the spermatogonia (green arrow) and primary spermatocytes (yellow arrow) was not above background (Fig. 1C and D).

Similarly, low-magnification, dark field images of seminiferous tubules hybridized with antisense *TSKS* (Fig. 1E and F) revealed a concentration of grains over adluminal spermatids. The higher magnification (×400) views of seminiferous tubules hybridized with antisense *TSKS* in both bright-field, and dark field (Fig. 1G and H) showed post-meiotic expression of *TSKS* mRNA in mouse testis, as was the case for *TSSK2*. When sense labeling was conducted as a control, no signal above background was detected (data not shown).

Centriolar localization of TSKS in human testicular cells and spermatozoa

To obtain clues regarding the biological role of TSKS, the subcellular localization of TSKS in human testicular cells was studied by immunofluorescent staining of enzyme dissociated spermatogenic cells from human testis (Fig. 2). Human TSKS was detected in round spermatids (Fig. 2A), principally as small immunofluorescent dots at the base of the sperm head. Upon careful study at high magnification, instead of a single dot, two small dots, located close together, were observed in some spermatids (*e.g.* the spermatids indicated by green arrowheads). In early and late elongating spermatids, TSKS immunofluorescence reached a peak in intensity and in the size of the immunofluorescent areas (Fig. 2B), which now comprised ovate structures, 2-3.5 μm in diameter located at the bases of the condensing spermatid nuclei. Often these structures appeared to be segmented into two parts. TSKS immunofluorescence subsequently declined in intensity and in size in testicular sperm, again showing two small, distinct dots at the base of the nucleus (Fig. 2C).

The staining of TSKS in the neck in spermatids and sperm suggested that TSKS might be localized to the redundant nuclear envelope, calreticulin containing vesicles, or the centrioles of human sperm. TSKS proteins did not co-localize with the SPANX or calreticulin proteins (data not shown), which are markers for the redundant nuclear envelope and calreticulin containing vesicles, respectively, in the cytoplasmic expansion of the sperm neck (Westbrook *et al.* 2001, Naaby-Hansen *et al.* 2001). To test if TSKS localized at the sperm centriole/basal body, three marker proteins were employed: γ-tubulin; α-tubulin; and a newly established centrosomal protein, Cep57 (KIAA 0092), which was discovered by proteomic analysis of human centrosomes and confirmed as a genuine centrosomal protein by correlation with known centrosomal proteins and by *in vivo* localization (Andersen *et al.* 2003). Moreover, the antibody

against Cep57 developed by Momotani *et al.* (2006) localized human Cep57 to centriolar pairs in mammalian somatic cell lines, suggesting that Cep57 is more specifically a centriolar protein (Momotani *et al.* personal communication). Using this antibody, two tiny Cep57 spots were detected in the human sperm neck (red color, Fig. 3B), which perfectly overlapped with TSKS positive spots (green color, Fig. 3A) and showed the yellow signal indicative of precise alignment in merged images (Fig. 3C), indicating that TSKS localized to the pair of centrioles.

A γ-tubulin antibody (mouse monoclonal anti-γ-tubulin, Abcam, Cat# ab11316) detected ~50 kDa sperm γ-tubulin by Western blot analysis (data not shown). Co-localization of TSKS and γ-tubulin revealed that the two small dots stained by anti-TSKS antibody (Fig. 3D, green color) were also recognized by anti γ-tubulin monoclonal antibody (red color, Fig. 3E). The precise alignment of yellow signal in the merged images of the dots (Fig. 3F) indicated co-localization of TSKS with γ-tubulin in the centrioles.

Staining of α-tubulin in human sperm using monoclonal α-tubulin antibody (Sigma, mouse monoclonal DM1A) is also shown in Fig. 3H. This immunoreagent stained two spots located at the apex (indicated by arrows) of the long α-tubulin signals from the axonemal microtubules. Once again, these spots co-localized with the staining produced by the TSKS antibody (Fig. 3G), and the precise yellow signal in the merged images (Fig. 3I) confirmed that TSKS localized at the centrioles. Thus, three independent centrosome/centriole marker proteins confirmed that TSKS is localized and concentrated in the pair of centrioles in human sperm. Further ultrastructural studies are required to precisely localize TSKS within the cylindrical centrioles themselves or in the pericentriolar material.

Overlap of TSKS and TSSK2 domains in human sperm

As shown in Fig. 4E, in addition to the strong and predominant TSKS signal detected in sperm centrioles (green color, indicated by arrows and enlarged in inset image), a fainter TSKS staining was also evident in the sperm tail, especially in the proximal midpiece region. After *in vitro* capacitation and the acrosome reaction, TSKS immunofluorescence persisted in both the centriolar and midpiece locations (data not shown).

Immunofluorescence localization of TSSK2 (Fig. 4B) revealed this kinase in the sperm neck (yellow arrows), the proximal midpiece of the sperm tail, and the equatorial segment (green arrowheads). The staining in the sperm neck was the most intense followed by the equatorial segment. The neck staining of TSSK2 overlapped with the region of TSKS staining and included the centrioles/basal body. However, the broader localization of TSSK2 in the equatorial segment, beyond the more restricted staining observed for TSKS in the tail, is intriguing and implies that additional substrates of TSSK2 may exist. Following *in vitro* capacitation and the acrosome reaction, the staining pattern of TSSK2 did not change. This indicated that TSSK2's association with the equatorial segment is not altered by acrosomal exocytosis and suggests roles for TSSK2 in maintenance of the equatorial segment after the acrosome reaction and possible transmission of TSSK2 to the egg after fertilization.

Dynamic changes in the subcellular localization of TSKS and TSSK2 during mouse spermiogenesis

Enzyme-disassociated mouse testicular cells were employed to analyze TSKS localization during mouse spermatogenesis, when dynamic changes occurred in its subcellular location (Fig. 5). TSKS (green signal) was not detected in primary spermatocytes or in step 1-6 round spermatids (Fig. 5A and B). TSKS staining was first noted as two prominent dots in the cytoplasm of step 10-14 spermatids (Fig. 5C) underlying the condensing nucleus. Precise co-localization of TSKS and γ-tubulin within these dots indicated that TSKS was localized in the paired centrioles in elongating mouse spermatids (Fig. 6). In step 15-16 spermatids, TSKS

positive dots were observed within the residual cytoplasm, and were later shed from testicular sperm in residual bodies (Fig. 5F). These observations are consistent with the degeneration of both centrioles known to occur during mouse spermatogenesis (Manandhar *et al.* 2005). In addition to the centriolar localization, TSKS immunofluorescence was also noted along the entire length of the flagellum in step 15-16 spermatids (Fig. 5D and E).

In dissociated mouse testicular cells TSSK2 was also detected in the cytoplasm of elongating spermatids, and a strong TSSK2 signal was found in the residual bodies, indicating that a subpopulation of TSSK2 is removed from the sperm with residual body shedding (data not shown). When studies of cryosections were conducted (Fig. 7), TSSK2 protein was mainly detected in post-meiotic spermatids within the cytoplasm of elongating and elongated spermatids (Fig. 7A and B) while dot-like TSSK2 signals were found in the residual bodies (Fig. 7C, shown by arrow), identified by their lack of nucleoli, confirming that a subpopulation of TSSK2 was removed from the developing spermatids when the residual bodies were shed. A strong signal for TSSK2 was found in flagella and heads of sperm in the epididymal lumen (Fig. 7D), which is consistent with the result from Western analysis that TSSK2 persists in mature mouse sperm (Xu *et al.* the companion paper).

Co-localization of TSSK2 and TSKS in mature mouse spermatozoa

Immunofluorescence microscopy of mouse epididymal sperm using antisera against TSSK2 and TSKS co-localized both proteins in middle and principal pieces of the flagellum and in the acrosomal region (Fig. 8A and D, yellow arrows indicate the acrosomal region). After *in vitro* induced capacitation, this staining pattern remained (Fig. 8B and E). However, after induction of the acrosome reaction *in vitro*, the acrosomal staining of both TSSK2 and TSKS disappeared, while the flagellar staining persisted (Fig. 8C and F). This indicated that a population of TSKS and TSSK2 associates with the acrosomal vesicle in mouse sperm and is lost with exocytosis. On the other hand, the persistence of flagellar staining for TSSK2 and TSKS in acrosome-reacted sperm suggests that these proteins may have important flagellar functions.

Discussion

Role of TSKS/TSSK2 in flagellogenesis

In situ hybridization revealed that mRNAs for TSSK2 and TSKS are expressed in spermatids. In both human and mouse spermatids TSKS protein localized to the centrioles during spermiogenesis where it reached its peak intensity during the period of flagellogenesis. During human spermatogenesis TSKS centriolar expression reached its highest expression level in elongating spermatids. In mice, mouse TSKS localized in spermatid centrioles at steps 10-15, and TSKS also persisted along the flagella of steps 15-16, but a population of TSKS was shed in residual bodies concurrent with centriolar reduction. These temporal expression patterns of TSKS, along with the arrested spermiogenesis observed in TSSK 1 & 2 chimeras (Xu *et al.* the companion paper), lead to the hypothesis that TSKS/TSSK2 is crucial to flagellar formation and function.

The steps in which TSKS expression is at maximal level are those in which microtubules form the manchette and assemble the flagellar axoneme, and actin and γ-tubulin also reach their peak expression (Tachibana *et al.* 2005). These temporal correlations suggest that TSKS/TSSK2 may be associated with dynamic changes in assembly of microtubule structures during spermiogenesis. Although we tested potential interactions of TSKS/TSSK2 with actin, α-tubulin and γ-tubulin by co-immunoprecipitation and no direct interactions were detected (data not shown), indirect interaction of TSKS/TSSK2 with cytoskeletal elements of centrioles and the axoneme may be mediated by other binding partners and needs further study.

It is also noteworthy that during flagellar formation the processes of intramanchette transport (IMT) and intraflagellar transport (IFT) are active (Marshall 2007). The current model suggests that IFT/IMT deliver building blocks from the manchette to the centrosome and then onward into the flagellum for assembling the sperm tail. The basal body/centriole thus is posited to function as a gathering point or "train station" for flagellar assembly factors during flagellum/cilium elongation (Deane *et al.* 2001, Rosenbaum and Witman 2002, Marshall 2007). In this regard the centrosome may be seen as a site for assembly of functional proteins (Kierszenbaum 2002). The kinases associated with the centrosome could provide modifications to the "cargo" proteins and/or the motors of IFT/IMT system, which are known to undergo protein phosphorylation (Burghoorn *et al.* 2007). It has been observed in mouse that IFT is involved in assembly of the mammalian sperm flagellum (San Agustin *et al.* 2001, 2002), however after completion of flagellar elongation, IFT disappeared (San Agustin, Pazour and Witman, personal communication) and the centrosome is reduced. TSSK2 may be recruited to the spermatid centriole through binding with TSKS, and play a role in phosphorylation of "cargo" proteins and/or the motors of IFT/IMT during flagellar formation.

TSKS, a marker protein of centrosome reduction during spermiogenesis

Complete centriolar degeneration has been observed in rodent spermatozoa, while only partial degeneration occurs in non-rodent species (Manandhar *et al.* 1998). Centrosome reduction during spermiogenesis includes the loss of microtubule nucleating function, loss of centrosomal proteins, and disintegration of centrioles (Manandhar *et al.* 2005). In ejaculated human sperm the immunofluorescent signals for TSKS persisted in both centrioles. By contrast, TSKS was absent in the centriolar region of mouse epididymal spermatozoa, consistent with the lack of centrioles in mature mouse spermatozoa, and at least some of the mouse TSKS was shed into residual bodies during spermiogenesis. Thus, TSKS provides a marker protein for studies of subcellular organelle(s) or compartments involved in centriole reduction during rodent spermiogenesis. The striking decline in mouse epididymal sperm of the ~60kDa TSKS isoform prominent in mouse testis and the dominance of the truncated ~40 kDa TSKSt isoform in mouse epididymal sperm (Xu *et al.* the companion paper), suggests that TSKS may undergo proteolysis during centrosome/centriole degeneration in mice. This raises the possibility that the truncated TSKS, TSKSt, may be a biochemical marker of centriolar degeneration in rodents and suggests that active proteolysis plays a role in this process.

Role of TSKS/TSSK2 in sperm motility and fertilization

TSSK2 and TSKS persist in human and mouse spermatozoa. In ejaculated human sperm, where the centrioles persist, TSSK2 and TSKS co-localized in neck and proximal midpiece regions while TSSK2 additionally localized to the equatorial segment, where it was unaffected by acrosomal exocytosis. In mouse sperm, a model in which centriolar degeneration occurs, TSSK2 and TSKS also persist in the flagellum, although they show no centriolar concentration. The persistence of both TSSK2 and TSKS in flagella of both human and mouse suggests that these proteins may be important for basic flagellar functions, including the possibility that TSSK2/TSKS might play a role in sperm motility by association with motility motors. Additionally, the fate of TSKS and TSSK2 following fertilization may be an important subject for further study. If the TSSK2/TSKS kinase/substrate pair do persist in the sperm centrioles and are released into the ooplasm during human fertilization, they may have some function to play in aster formation in early cleavage, an event thought to be directed by the sperm centrioles.

TSKS/TSSK2, a coiled-coil protein/ kinase pair

Two coiled-coil regions lie within TSKS at aa 147-234, and aa 324-392, respectively. The N-terminus of TSKS rather than these coiled-coil regions appears to be responsible for binding

with TSSK2 (Xu *et al.* the companion paper). These coiled-coil regions, however, may be important for anchoring TSKS to the spermatid centriole.

Centrosomal coiled-coil proteins and their interaction with kinases have drawn special attention in recent years. It is known that some coiled-coil proteins self-assemble or assemble with other coiled-coil proteins, and through this assembly, the coiled-coil proteins form the fibrillar structure of the centrosome (Donkor *et al.* 2004). It is also known that some coiled-coil proteins require protein phosphorylation/dephosphorylation at specific residues to associate at the centrosome (Fabbro *et al.* 2005). The centrosomal coiled-coil proteins then recruit correlated kinases to achieve multiple centrosomal functions (Gillingham and Munro 2000). A well studied model is ODF2/Plk1 pair. ODF2 is a major protein of sperm tail outer dense fibers and also a central component of the centrosomal scaffold in somatic cells (Nakagawa *et al.* 2001). Its coiled-coil regions may be responsible for forming a fibrillar structure by self-association. Direct interaction of a somatic splice variant of ODF2, hCenexine, with the mammalian polo-like kinase 1 (Plk1) has been demonstrated. The unique C-terminal extension of hCenexine, which is absent from sperm ODF2, is required for proper recruitment of Plk1 as well as other centrosomal components crucial for normal mitosis in human somatic cell lines (Soung *et al.* 2006).

TSKS/TSSK2 is the first coiled-coil protein/kinase pair studied and localized in the gamete centriole. We have demonstrated that the N-terminus of TSKS strongly binds with TSSK2 (Xu *et al.* the companion paper). Thus, we propose that TSKS targets to the centriole through coiled-coil region interactions and that the centriolar localization depends on a specific phosphorylation by TSSK2, which may be recruited to the centriole through binding the N-terminus of TSKS.

In summary, the cellular concentration of the TSSK2 enzyme in the sperm neck and the localization of its substrate, TSKS, at the centriole imply roles in flagellar biogenesis and sperm motility. This subcellular localization is in accord with the infertile phenotype of TSSK1 & 2 chimeras due to haploinsufficiency with affected testes arrested in spermatogenesis (Xu *et al.* the companion paper). The targeting deletion of TSKS will be the next step studying further studies of the function of this kinase/substrate pair in the spermatid centriole.

Acknowledgements

We thank Dr. Robert A. Bloodgood and Dr. Jeffrey J. Lysiak and others at the Center for Research in Contraceptive and Reproductive Health for critique of the manuscript. This work was supported in part by NIH R03 HD055129, R01 HD 045783, R01 HD037416, NIH Fogarty International Center Grant D43 TW/HD 00654, NIH U54 HD29099, the Andrew W. Mellon Foundation and Schering AG.

References

Andersen JS, Wilkinson CJ, Mayor T, Mortensen P, Nigg EA, Mann M. Proteomic characterization of the human centrosome by protein correlation profiling. Nature 2003;426:570–4. [PubMed: 14654843]

Barros TP, Kinoshita K, Hyman AA, Raff JW. Aurora A activates D-TACC-Msps complexes exclusively at centrosomes to stabilize centrosomal microtubules. J Cell Biol 2005;170:1039–46. [PubMed: 16186253]

Burghoorn J, Dekkers MP, Rademakers S, de Jong T, Willemsen R, Jansen G. Mutation of the MAP kinase DYF-5 affects docking and undocking of kinesin-2 motors and reduces their speed in the cilia of Caenorhabditis elegans. Proc Natl Acad Sci U S A 2007;104:7157–62. [PubMed: 17420466]

Cowan CR, Hyman AA. Cyclin E-Cdk2 temporally regulates centrosome assembly and establishment of polarity in Caenorhabditis elegans embryos. Nat Cell Biol 2006;8:1441–7. [PubMed: 17115027]

Deane JA, Cole DG, Seeley ES, Diener DR, Rosenbaum JL. Localization of intraflagellar transport protein IFT52 identifies basal body transitional fibers as the docking site for IFT particles. Curr Biol 2001;11:1586–90. [PubMed: 11676918]

Donkor FF, Monnich M, Czirr E, Hollemann T, Hoyer-Fender S. Outer dense fibre protein 2 (ODF2) is a self-interacting centrosomal protein with affinity for microtubules. J Cell Sci 2004;117:4643–51. [PubMed: 15340007]

Fabbro M, Zhou BB, Takahashi M, Sarcevic B, Lal P, Graham ME, Gabrielli BG, Robinson PJ, Nigg EA, Ono Y, Khanna KK. Cdk1/Erk2- and Plk1-dependent phosphorylation of a centrosome protein, Cep55, is required for its recruitment to midbody and cytokinesis. Dev Cell 2005;9:477–88. [PubMed: 16198290]

Fawcett DW. A comparative view of sperm ultrastructure. Biol Reprod 1970;2:90–127. [PubMed: 5521054]

Fry AM, Mayor T, Meraldi P, Stierhof YD, Tanaka K, Nigg EA. C-Nap1, a novel centrosomal coiled-coil protein and candidate substrate of the cell cycle-regulated protein kinase Nek2. J Cell Biol 1998;141:1563–74. [PubMed: 9647649]

Giet R, McLean D, Descamps S, Lee MJ, Raff JW, Prigent C, Glover DM. Drosophila Aurora A kinase is required to localize D-TACC to centrosomes and to regulate astral microtubules. J Cell Biol 2002;156:437–51. [PubMed: 11827981]

Gillingham AK, Munro S. The PACT domain, a conserved centrosomal targeting motif in the coiled-coil proteins AKAP450 and pericentrin. EMBO Rep 2000;1:524–9. [PubMed: 11263498]

Hamill DR, Severson AF, Carter JC, Bowerman B. Centrosome maturation and mitotic spindle assembly in C. elegans require SPD-5, a protein with multiple coiled-coil domains. Dev Cell 2002;3:673–84. [PubMed: 12431374]

Hao Z, Jha KN, Kim YH, Vemuganti S, Westbrook VA, Chertihin O, Markgraf K, Flickinger CJ, Coppola M, Herr JC, Visconti PE. Expression analysis of the human testis-specific serine/threonine kinase (TSSK) homologues. A TSSK member is present in the equatorial segment of human sperm. Mol Hum Reprod 2004;10:433–44. [PubMed: 15044604]

Hong YR, Chen CH, Chang JH, Wang S, Sy WD, Chou CK, Howng SL. Cloning and characterization of a novel human ninein protein that interacts with the glycogen synthase kinase 3beta. Biochim Biophys Acta 2000;1492:513–6. [PubMed: 11004522]

Jha KN, Salicioni AM, Arcelay E, Chertihin O, Kumari S, Herr JC, Visconti PE. Evidence for the involvement of proline-directed serine/threonine phosphorylation in sperm capacitation. Mol Hum Reprod 2006;12:781–9. [PubMed: 17050774]

Keller LC, Romijn EP, Zamora I, Yates JR 3rd, Marshall WF. Proteomic analysis of isolated chlamydomonas centrioles reveals orthologs of ciliary-disease genes. Curr Biol 2005;15:1090–8. [PubMed: 15964273]

Kemp CA, Kopish KR, Zipperlen P, Ahringer J, O'Connell KF. Centrosome maturation and duplication in C. elegans require the coiled-coil protein SPD-2. Dev Cell 2004;6:511–23. [PubMed: 15068791]

Keryer G, Witczak O, Delouvee A, Kemmner WA, Rouillard D, Tasken K, Bornens M. Dissociating the centrosomal matrix protein AKAP450 from centrioles impairs centriole duplication and cell cycle progression. Mol Biol Cell 2003;14:2436–46. [PubMed: 12808041]

Kierszenbaum AL. Spermatid manchette: plugging proteins to zero into the sperm tail. Mol Reprod Dev 2001;59:347–9. [PubMed: 11468770]

Kierszenbaum AL. Intramanchette transport (IMT): managing the making of the spermatid head, centrosome, and tail. Mol Reprod Dev 2002;63:1–4. [PubMed: 12211054]

Kueng P, Nikolova Z, Djonov V, Hemphill A, Rohrbach V, Boehlen D, Zuercher G, Andres AC, Ziemiecki A. A novel family of serine/threonine kinases participating in spermiogenesis. J Cell Biol 1997;139:1851–9. [PubMed: 9412477]

Le Bot N, Tsai MC, Andrews RK, Ahringer J. TAC-1, a regulator of microtubule length in the C. elegans embryo. Curr Biol 2003;13:1499–505. [PubMed: 12956951]

Manandhar G, Schatten H, Sutovsky P. Centrosome reduction during gametogenesis and its significance. Biol Reprod 2005;72:2–13. [PubMed: 15385423]

Manandhar G, Simerly C, Schatten G. Centrosome reduction during mammalian spermiogenesis. Curr Top Dev Biol 2000a;49:343–63. [PubMed: 11005027]

Manandhar G, Simerly C, Schatten G. Highly degenerated distal centrioles in rhesus and human spermatozoa. Hum Reprod 2000b;15:256–63. [PubMed: 10655294]

Manandhar G, Sutovsky P, Joshi HC, Stearns T, Schatten G. Centrosome reduction during mouse spermiogenesis. Dev Biol 1998;203:424–34. [PubMed: 9808791]

Marshall WF. What is the function of centrioles? J Cell Biochem 2007;100:916–22. [PubMed: 17115414]

Momotani, K.; Khromov, A.; Miyake, T.; Somlyo, A.; Stukenberg, T.; Somlyo, A. A novel centrosome protein involved in regulation of microtubule formation. Poster presented at an annual meeting of Professional Research Scientists (Experimental Biology 2006); San Francisco, California. 2006.

Naaby-Hansen S, Wolkowicz MJ, Klotz K, Bush LA, Westbrook VA, Shibahara H, Shetty J, Coonrod SA, Reddi PP, Shannon J, Kinter M, Sherman NE, Fox J, Flickinger CJ, Herr JC. Co-localization of the inositol 1,4,5-trisphosphate receptor and calreticulin in the equatorial segment and in membrane bounded vesicles in the cytoplasmic droplet of human spermatozoa. Mol Hum Reprod 2001;7:923–33. [PubMed: 11574661]

Nakagawa Y, Yamane Y, Okanoue T, Tsukita S, Tsukita S. Outer dense fiber 2 is a widespread centrosome scaffold component preferentially associated with mother centrioles: its identification from isolated centrosomes. Mol Biol Cell 2001;12:1687–97. [PubMed: 11408577]

Nakamura S, Terada Y, Rawe VY, Uehara S, Morito Y, Yoshimoto T, Tachibana M, Murakami T, Yaegashi N, Okamura K. A trial to restore defective human sperm centrosomal function. Hum Reprod 2005;20:1933–7. [PubMed: 15831510]

Rosenbaum JL, Witman GB. Intraflagellar transport. Nat Rev Mol Cell Biol 2002;3:813–25. [PubMed: 12415299]

San Agustin JT, Pazour GJ, Witman GB. Intraflagellar transport is essential for mammalian sperm tail formation. Mol Biol Cell 2001;12:446a.

San Agustin JT, Pazour GJ, Witman GB. A defect in intraflagellar transport (IFT) in mice leads to resorption of aberrant spermatids, apoptotic death of spermatocytes, and sterility. Mol Biol Cell 2002;13:190a.

Schatten G. The centrosome and its mode of inheritance: the reduction of the centrosome during gametogenesis and its restoration during fertilization. Dev Biol 1994;165:299–335. [PubMed: 7958403]

Sillibourne JE, Milne DM, Takahashi M, Ono Y, Meek DW. Centrosomal anchoring of the protein kinase CK1delta mediated by attachment to the large, coiled-coil scaffolding protein CG-NAP/AKAP450. J Mol Biol 2002;322:785–97. [PubMed: 12270714]

Soung NK, Kang YH, Kim K, Kamijo K, Yoon H, Seong YS, Kuo YL, Miki T, Kim SR, Kuriyama R, Giam CZ, Ahn CH, Lee KS. Requirement of hCenexin for proper mitotic functions of polo-like kinase 1 at the centrosomes. Mol Cell Biol 2006;26:8316–35. [PubMed: 16966375]

Stoler MH. In situ hybridization. Clin Lab Med 1990;10:215–36. [PubMed: 1691963]

Sutovsky P, Schatten G. Paternal contributions to the mammalian zygote: fertilization after sperm-egg fusion. Int Rev Cytol 2000;195:1–65. [PubMed: 10603574]

Tachibana M, Terada Y, Murakawa H, Murakami T, Yaegashi N, Okamura K. Dynamic changes in the cytoskeleton during human spermiogenesis. Fertil Steril 2005;84:1241–8. [PubMed: 16210017]

Westbrook VA, Diekman AB, Naaby-Hansen S, Coonrod SA, Klotz KL, Thomas TS, Norton EJ, Flickinger CJ, Herr JC. Differential nuclear localization of the cancer/testis-associated protein, SPAN-X/CTp11, in transfected cells and in 50% of human spermatozoa. Biol Reprod 2001;64:345–58. [PubMed: 11133693]

Wigge PA, Jensen ON, Holmes S, Soues S, Mann M, Kilmartin JV. Analysis of the Saccharomyces spindle pole by matrix-assisted laser desorption/ionization (MALDI) mass spectrometry. J Cell Biol 1998;141:967–77. [PubMed: 9585415]

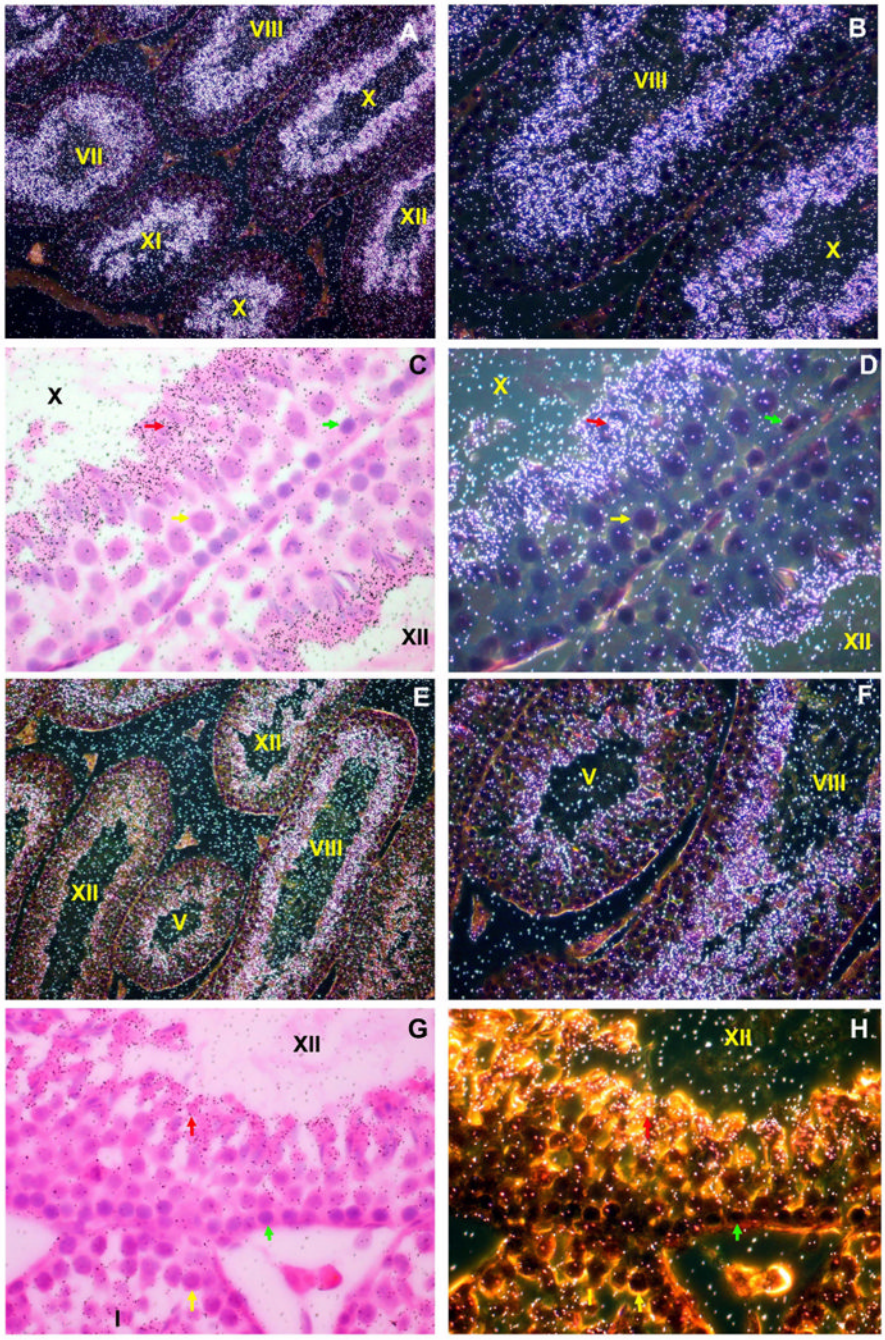

Figure 1. Analysis of *TSSK2* and *TSKS* mRNA expression in adult mouse testis

In situ hybridization of *TSSK2* (A-D) and *TSKS* (E-H) transcripts with radiolabeled mouse *TSSK2* and *TSKS* cRNAs. The low-magnification (×100-200) views of seminiferous tubules hybridized with antisense *TSSK2* (A, B) are shown in dark field with higher magnifications (×400) shown in both bright field (C), and dark field (D). *TSSK2* transcripts were expressed mainly in post-meiotic spermatids. The low-magnification (×100-200) views of seminiferous tubules hybridized with antisense *TSKS* (E, F) are shown in dark field, while the higher magnification (×400) views of seminiferous tubules hybridized with antisense *TSKS* are also shown in both bright field (G), and dark field (H). *TSKS* transcripts were also expressed mainly

in the post-meiotic spermatids. Primary spermatocytes are indicated with yellow arrows, spermatogonia with green arrows, and spermatids with red arrows.

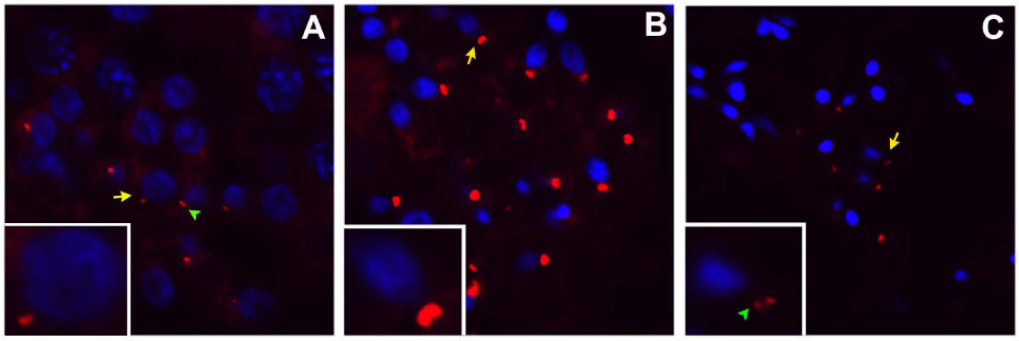

Figure 2. Immunofluorescent staining of TSKS in disassociated cells from human testis

TSKS (red signal) was first detected in round spermatids where one or two small fluorescent spots were evident at the base of the nucleus (A). Both intensity and size of the fluorescent signal for TSKS peaked in elongating spermatids (B). The TSKS signal subsequently declined in more mature testicular spermatids (C). Insets show enlarged spermatids noted by yellow arrows at low magnification. Green arrowheads in A and C indicate sperm with two distinct spots. The nuclei were counterstained with DAPI (blue signal).

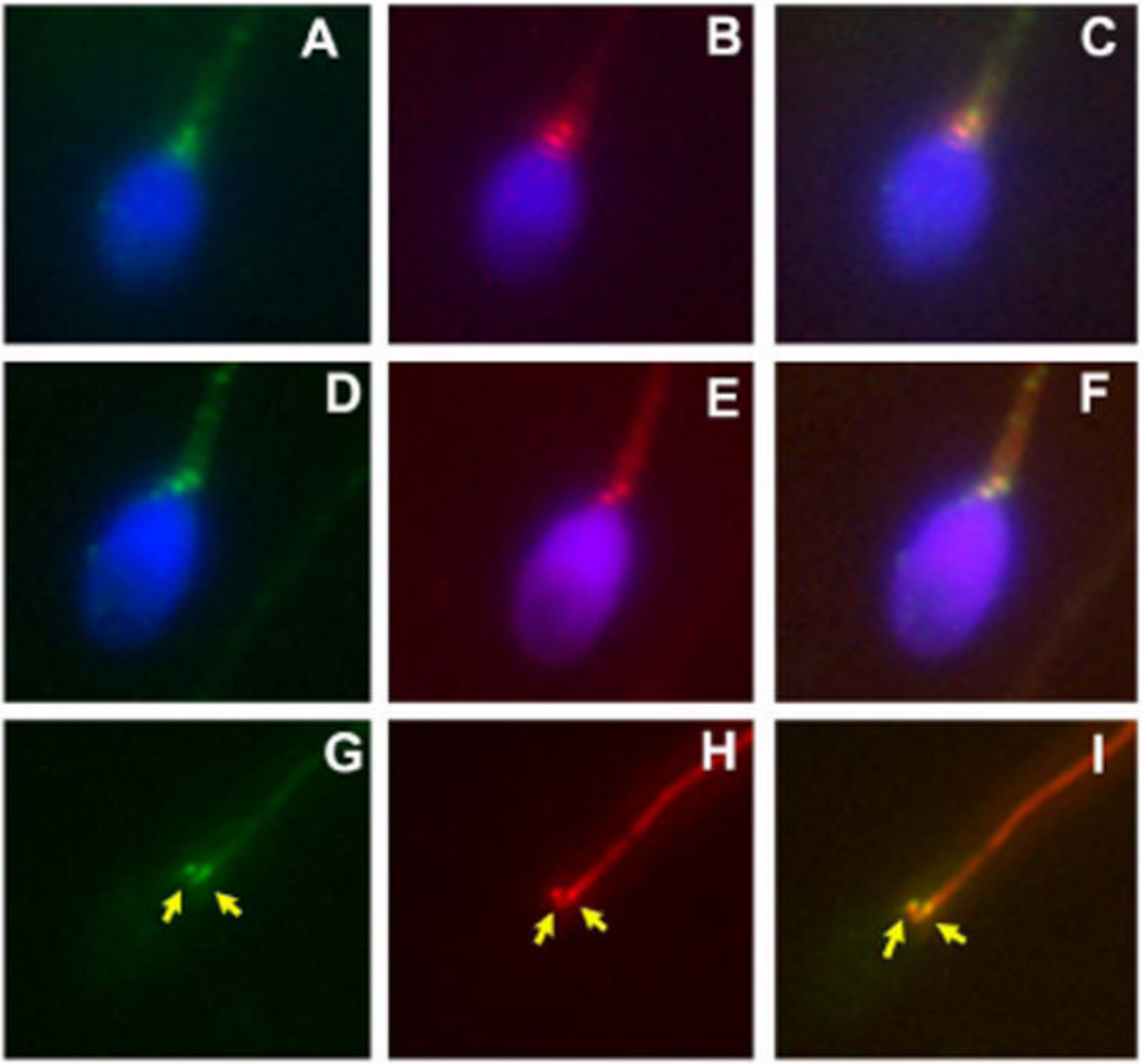

Figure 3. Co-localization of TSKS with centrosome/centriole marker proteins in human spermatozoa

A-C: Immunofluorescent staining of TSKS (A) and Cep57 (B) with overlay images of A and B (C) are shown. D-F: Immunofluorescence staining of TSKS (D) and γ-tubulin (E) are presented with overlay images of D and E (F). G-I: Immunofluorescence staining of TSKS (G), α-tubulin (H) is shown with overlay image of G and H (I). Yellow color in the overlay images indicates precise co-localization of TSKS with Cep57, γ-tubulin and α-tubulin localizing TSKS in the human sperm centrioles.

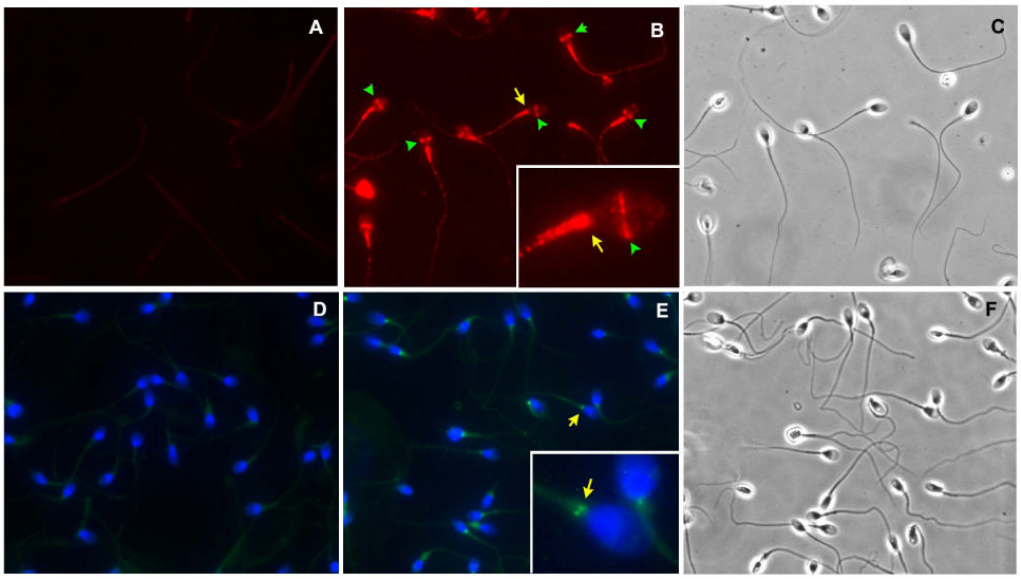

Figure 4. Immunofluorescent localization of TSSK2 and TSKS in ejaculated "swim-up" human spermatozoa

Sperm were stained with pre-immune control (A) and red anti-TSSK2 (B), or with pre-immune control (D) and green anti-TSKS (E). C and F are phase contrast images of B and E. In D and E, the nuclei are counterstained with DAPI (blue color). Insets in B and E show enlargements of the sperm indicted with arrows. TSSK2 (B) was localized in the neck (yellow arrows) and proximal midpiece and additionally in the equatorial segment (green arrowheads). TSKS (E) concentrated in the paired centioles (yellow arrows).

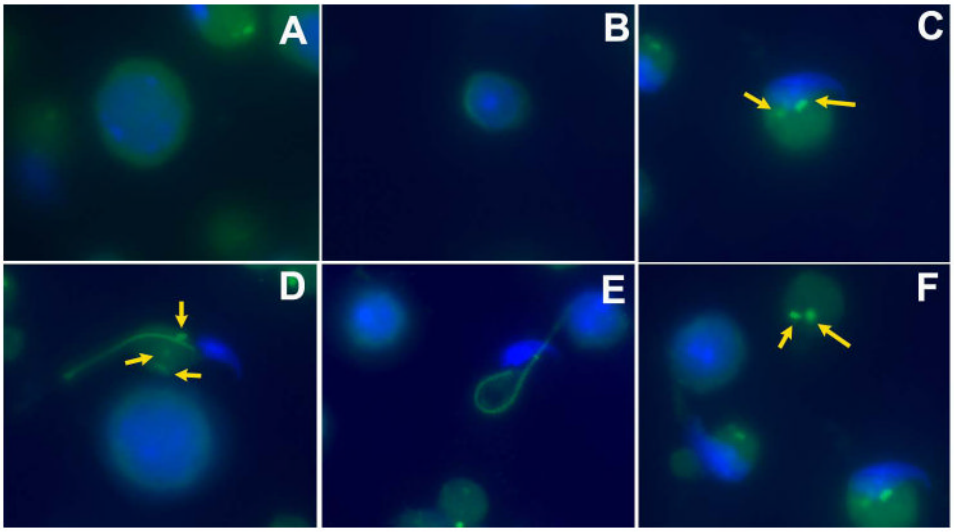

Figure 5. Immunofluorescent staining of TSKS in enzyme-disassociated cells from mouse testis

TSKS (green signal) was not detected in primary spermatocytes (A) or step 1-6 round spermatids (B). TSKS proteins were first noted as two prominent dots in the cytoplasm of steps 10-14 spermatids (C arrows) beneath the condensing nucleus. TSKS proteins were present in the cytoplasm as prominent dots (arrows) and then appeared along the entire flagellum of steps 15-16 spermatids (D). The TSKS positive dots were shed from some testicular sperm in steps 15-16 spermatids while TSKS localization along the entire tail persisted (E). The TSKS positive dots (arrows) were detected in the residual bodies, which were shed form testicular sperm and identified by the absence of nuclear staining (F). Control staining using the pre-immune serum was negative (data not shown). The nuclei were counterstained with DAPI (blue color).

Figure 6. Co-localization of TSKS with the centrosomal protein marker γ-tubulin in mouse spermatids

Immunofluorescence staining of TSKS (A) and γ-tubulin (B) with overlay images of A and B (C) in elongating spermatids are shown. This precise co-localization of TSKS with γ-tubulin indicated that TSKS is present in the paired centrioles in elongating spermatids at steps 10-14.

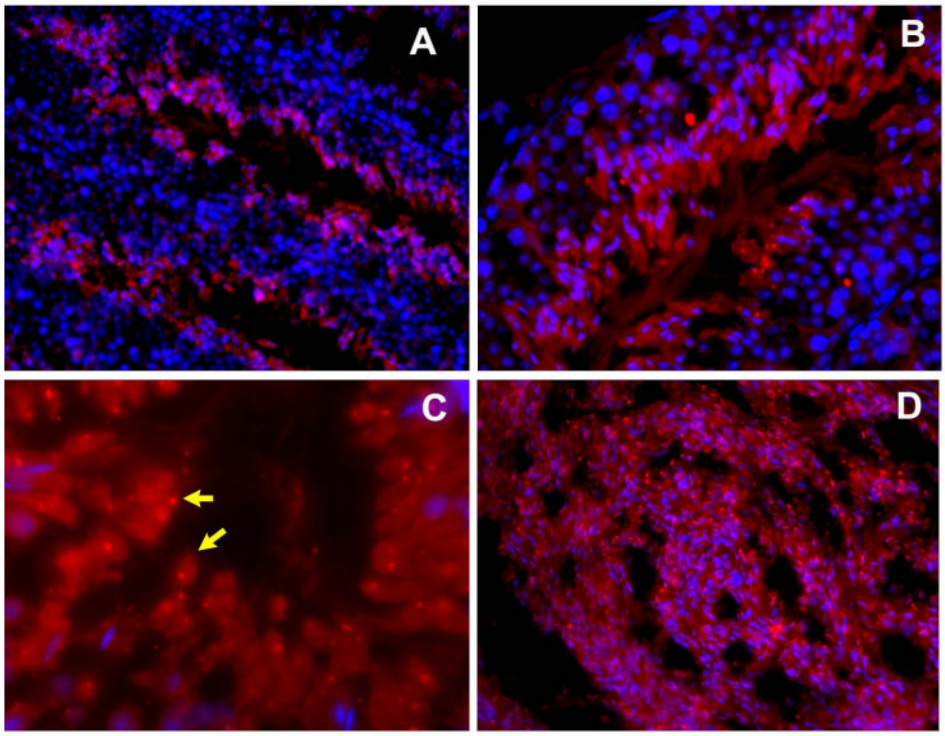

Figure 7. Immunofluorescent localization of TSSK2 in cryosections of mouse testes and epididymides

In mouse testes (A-B) TSSK2 protein was detected in adluminal post-meiotic elongating and elongated spermatids, while dot-like TSSK2 signals were found in the residual bodies (C, shown by arrows), identified by their lack of nucleoli. A strong TSSK2 signal was found in sperm in the epididymal lumen (D). The nuclei were counterstained with DAPI (blue signal).

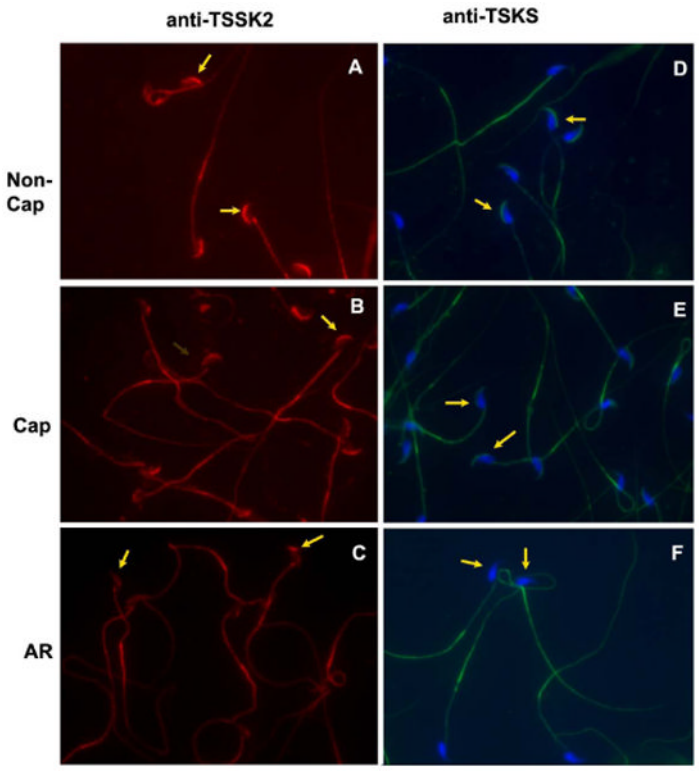

Figure 8. Immunofluorescent localization of TSKS and TSSK2 in mouse epididymal spermatozoa

Non-capacitated epididymal spermatozoa (Non-cap, A and D), capacitated spermatozoa (Cap, B and E) and acrosomal-reacted spermatozoa (AR, C and F) were stained with anti-TSSK2 (A, B, C) and anti-TSKS (D, E, F). Immunofluorescent staining of TSSK2 (A) and TSKS (D) was detected in the acrosomal region (yellow arrows) and along the entire flagella of mouse epididymal spermatozoa. The TSSK2 and TSKS expression pattern did not change after *in vitro* capacitation (B, E). The acrosomal localization of both TSSK2 and TSKS diminished (yellow arrows) after *in vitro* acrosome reaction, while the flagellar localization persisted (C, F).